Macromolecules

Article

pubs.acs.org/Macromolecules

Probing the Mesh Formed by the Semirigid Polyelectrolytes

K. Salamon,[†] D. Aumiler,[†] G. Pabst,[‡] and T. Vuletić*,[†]

[†]Institut za fiziku, Bijenička 46, 10000 Zagreb, Croatia

[‡]University of Graz, Institute of Molecular Biosciences, Biophysics Division, Schmiedlstr. 6, 8042 Graz, Austria

Supporting Information

ABSTRACT: We correlate conformation and dynamics of the semirigid polyelectrolytes deoxyribonucleic acid (DNA) and hyaluronic acid (HA) in the semidilute regime, across a broad concentration range (10^{-3} – 10^{2} g/L). Salt-free polyelectrolytes are distinct from uncharged polymers as they presumably form a rather rigid, isotropic mesh. The polyelectrolyte characteristic mesh size is known as de Gennes correlation length ξ. We directly probed the mesh formed by DNA and HA, by employing fluorescence correlation spectroscopy (FCS) to measure the diffusion coefficient of fluorescently labeled DNA fragments added in trace amounts. For the salt-free solutions we found that the DNA or HA mesh size has to be 2–3 times larger than the fragments for them to start to diffuse freely (as if in the dilute solution). For a tighter mesh (concentrations 0.1–1 g/L), the fragment diffusion coefficient is only half the free diffusion value. Conversely, fragments show the free diffusion coefficient—as if there is no mesh—in DNA or HA in 10 mM buffer. This complies well with the fact that the ξ fades for polyelectrolytes with added salt. The diffusion coefficient falls off further when the mesh size gets smaller than the fragment size (above 1 g/L) and a similar value is reached in buffer as well as in pure water, respectively, at the highest measured concentrations (10 g/L). We also performed small-angle X-ray scattering (SAXS) on HA and DNA (range 3–130 g/L) to complement our previous dielectric spectroscopy (DS) studies (range 0.01–5 g/L). Combined, these methods provide reference values of the de Gennes length ξ across the range studied by FCS.

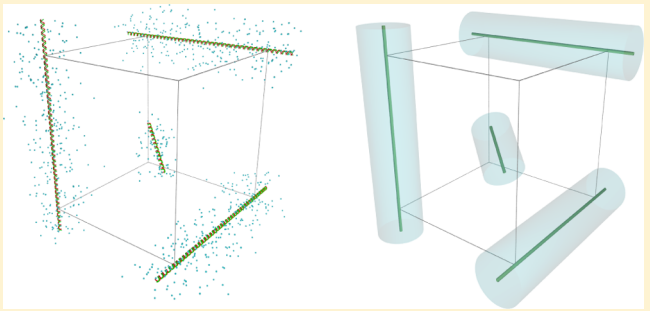

INTRODUCTION

Polyelectrolytes are polymers with ionizable groups on their constituent monomers. Therefore, they dissociate in polar solvents, such as water into polyions and a cloud of small counterions. The long-range Coulomb interaction among all these entities makes polyelectrolytes quite unlike uncharged polymers in aqueous solvents. The electrostatics leads both to distinctive technical applications and to difficulties in understanding these systems.[1−4]

Polyions, as well as polymers, depending on their rigidity can be modeled as ideal, freely jointed chains, as segmented (Kuhn) chains, as wormlike chains, or even as rod-like objects.[4] The polyion backbone, as a source of the potential for the ionic atmosphere can be modeled either as a linear charge, or a line of discrete charges, or as a 3D object (cylinder) with some charge distribution.[5] The strong electrostatic potential of the polyion may cause counterions to Manning condense on the polyion to reduce its effective charge.[6,7] In understanding the conformation of polyions and their arrangement in solution, the counterion atmosphere enters as a source of screening for the charges of the polyion backbone.[8,9] As such the polyion backbone rigidity may be strongly enhanced due to a lack of screening. The way the polyion is modeled also depends on the way the atmosphere is described: mean-field approximation, Poisson−Boltzmann, within the Debye−Hückel approximation or a nonlinear PB, or a nonmean-field approximation taking charge correlations into account.[10−12] Considering all the above, one should take into account the conformational properties of a single polyion, and the spatial arrangement of the polyion ensemble,[13] as well as the (radial) distribution of their ionic atmosphere.

Experiments on polyelectrolytes necessarily reflect effects of both components, polyions and the ionic cloud, all the while being designed to distinguish between the effects of the two contributions by, e.g., studying the polyion conformation in varying (counter)ion atmospheres,[14−16] or by studying the changes to the atmosphere that may occur with variation in polyion length, stiffnes or concentration.[17−19]

In this work we demonstrate how the dynamics of the complete polyion-counterion atmosphere system directly reflects the static conformation of polyions, and how the experimental approaches addressing either component may provide results on one and the same parameter—the de Gennes correlation length (mesh size).[20] The applied description of polyelectrolytes is based on the evaluation of different length scales which primarily depend on polyion and added salt concentrations (see Appendix A). A simple way to understand de Gennes length is that it is the characteristic size

Received: October 16, 2012
Revised: January 6, 2013
Published: January 28, 2013

of the mesh formed by the polyions in the solution. Quite often ξ is depicted as such,[8,17,21] as shown in Figure 1. We remind the

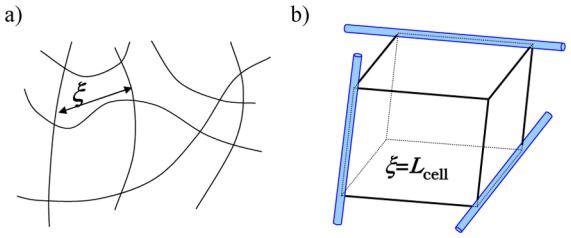

Figure 1. (a) Long overlapping chains form a semidilute solution, depicted[21] as a twodimensional, 2D polyion network, with correlation length/mesh size denoted as ξ. (b) Mesh cell delimited by three (for three directions in space) chains crossing each other. The size of such a cell is the mesh size of the polyion network in 3D.

reader, however, that such a simplified depiction of a mesh may apply also to a semidilute solution of uncharged polymers, while de Gennes length scale is characteristic of semidilute polyelectrolytes and is not experimentally observed for uncharged polymer solutions.

The physical meaning of a correlation length is that beyond this distance correlation between the polyion chain segments should vanish. This notion is used in conjunction with interpretations of the origin of the peak in the scattering curves.[22] The peak position q_m is considered to provide a direct measurement of the correlation length $\xi = 2\pi/q_m$. Koyama[23,24] has simulated scattering intensity of a polyelectrolyte. These curves featured a peak, when existence of a correlation hole was assumed. The hole represents a ξ region around the polyion segment where the probability that another segments will be found is negligible. The tendency for segments to stay at a distance is due to Coulomb repulsion. Besides the lack of the peak for uncharged polymers, this description is supported also by the suppression of the scattering peak with addition of salt to polyelectrolytes. Added salt screens the Coulomb repulsion of the segments—thus the correlation hole and the corresponding peak disappear[22,25]

The depiction of the mesh may be improved by introducing a third dimension, Figure 1b). We assume that, on average, three polyions for three directions in space, approach and cross each other and thus delimit a mesh cell of the polyion network. The size of the mesh cell L_{cell} may be interpreted as the average distance between the nearest-neighbor chain segments. Here, we take into account that a polyelectrolyte should be isotropic and homogeneous and that it does not show any long-range ordering. Indeed, very early it has been shown that polyelectrolytes do not form any ordered structure.[23] E.g., there should not be any domains where polyions stretch parallel to each other.[25] Oriented domains only occur at very high concentrations where liquid crystalline organization appears (for DNA, above 150−200 g/L).[26] Also, only a few polyions should cross each other within a given portion of space, and thus form a mesh cell. If this were not the case, local concentration would be enhanced, thus inducing reductions elsewhere, which would not lead to polyelectrolyte homogeneity.

The size L_{cell} is directly defined by the polyelectrolyte concentration. That is, the number of monomers found within the cell is $(1/4)((3L_{cell})/b)$, where b is the monomer size of the polyelectrolyte in question. A factor 1/4 enters as the polyions are found on the edges − so only a quarter of each is found within the cell. This number of monomers, when divided by the cell volume L_{cell}^3 gives the polyelectrolyte monomer concentration (number density) $n = 3/(4*b*(\mathrm{L\ cell})_2)$. Evidently, the mesh cell size or near-neighbor distance of chain segments in the mesh scales as expected for correlation length

$$L_{cell} \approx \xi \approx (bn)^{-1/2} \quad (1)$$

We note that these considerations apply best for the semirigid polyelectrolytes whose persistence length is longer than correlation length[21] and so, on the level of the cell, they behave as rigid rods. This condition may also be satisfied for flexible polyelectrolytes when there is no added salt, as the electrostatic contribution to the persistence length may be significant.[18,27] Locally rigid mesh is the least dense way to pack polyions in the solution—it allows for maximum distance of segments and a reduction in Coulomb interaction. For a flexible polyelectrolyte, relating the mesh size and concentration depends on how many monomers get *packed* into one electrostatic blob. That is, a more flexible polyelectrolyte, possibly with only a fraction of charged monomers, in a highly screening environment with added salt gets locally coiled into electrostatic blobs and behaves as a chain of such blobs.[9] For such a polyelectrolyte the above relationship between the monomer concentration and the mesh size is more ambiguous and maybe not even linear.[28]

In this work we relate the physical size of the mesh cell evidenced by fluorescence correlation spectroscopy (FCS) with the correlation length as obtained from small angle X-ray scattering (SAXS) and dielectric spectroscopy (DS, see Appendix B) experiments—and we ascertain the absolute values for this length scale in the conditions of no added salt, where the ionic atmosphere consists only of counterions that have dissociated from the polyion. In such a case electrostatic screening is reduced to a minimum and the long-range of electrostatic force emphasizes the distinctive nature of the polyelectrolytes compared to the uncharged polymers. In the opposite case of high added salt, screening renders polyelectrolytes with quite similar properties as those of uncharged polymers. This is a standard explanation for the routinely observed suppression of the polyelectrolyte peak in scattering curves.[22,24] Now, we show also by FCS that the polyion mesh dissappears in these conditions—that the polyions become uncorrelated. Here we note that application of optical techniques to measure diffusion, i.e., dynamics of molecules within rigid networks (actin network) has been reported quite some time ago by Sackmann et al..[13] Quasi-elastic light scattering was used for discerning dynamics of actin filaments and the mesh they form. However, FCS distinguishes itself by providing utmost distinction between the probe molecule and the mesh iself. It is well accepted for studies of crowded macromolecular environments.[29,30]

We study semirigid biopolyelectrolytes DNA and hyaluronic acid (HA, a polysaccharide) which have a rather large structural persistence length, ∼50 nm[31] and ∼10 nm,[27,32] respectively. This and very low added salt conditions ensure that the polyelectrolyte mesh is built by rodlike polyions which simplifies our considerations. For comparison, most synthetic polyelectrolytes, with their −C−C− backbone and monomer size of 0.25 nm have the structural persistence length comparable to this monomer size, and are considered as flexible. We report SAXS and FCS experiments on polydisperse DNA and HA, both in forms of sodium salts, at concentrations where these are in the semidilute regime. This study

dx.doi.org/10.1021/ma3021486 | Macromolecules 2013, 46, 1107−1118

complements our previous DS study of these samples,[18,33] as well as SAXS, DS and FCS studies of solutions of monodiperse, 150 bp mononucleosomal DNA fragments.[15,19,25,34] We include the static properties and dynamic responses—originating from different techniques that probe different components of the polyelectrolyte solution, in order to create a consistent picture of a fundamental length scale describing a polyelectrolyte as an ensemble.

EXPERIMENTAL METHODS

Materials. Solutions of deoxyribonucleic acid (DNA) and hyaluronic acid (HA), both in forms of sodium salts, were prepared in ultrapure water (Millipore Milli-Q), in most cases without addition of any simple salts or a buffer. Dissolution in pure water, without a buffer leads to a solution where pH is defined by CO_2 dissolved in water, and we get pH about 6. In these conditions both DNA (pK_a = 0) and HA (pK_a = 3.2[35]) are fully ionized. In the course of our previous studies[18,19,33,34] where we used DNA and HA samples described just below, we assured that the salt content in these samples is negligible, less than one added salt ion per 10 monomers. Dialysing or not the samples prior to use gave no discernible effect, so it was not attempted for this study. Thus, samples dissolved in pure water are taken to be free of added salt.

Salmon testes lyophilized DNA threads were obtained from Sigma-Aldrich (Cat. No. D1626). This DNA is polydisperse, with chain sizes in the range from 2 kbp to 20 kbp (contour length 0.7−7 μm) and presumably up to 200 kbp.[15,36] Hyaluronic acid sodium salt from *Streptococcus equi sp.* was obtained from Sigma-Aldrich (Cat. No. Fluka53747). The low protein content is declared by the manufacturer. An average molecular weight is about 1.63×10^6 Da, implying an average polymerizaton degree of 4000, or a contour length of 4 μm.[33,37]

Because the studied DNA and HA have rather long chain lengths, in the micrometer range, the corresponding dilute-semidilute crossover concentrations are expected to be several orders of magnitude below the concentration range we studied.[14,17] Thus, these samples are certainly in the semidilute regime. We denote them as long DNA or HA.

In this paper, we will often refer to works[15,19,25,34] on mononucleosomal DNA fragments, prepared[38] by enzymatic digestion of H1-depleted calf thymus chromatin.[39] These highly monodisperse samples contain 150 ± 10 bp fragments (as checked by gel-electrophoresis) together with traces of 300−350 bp fragments that correspond to two nucleosomal DNA fragments connected by undigested linker DNA. Unlike micrometer-sized long DNA or HA, these fragments are only 50 nm long, and practically rod-like. As there are nominally 146bp of DNA wrapped in a nucleosome, we denote these samples DNA146.

The following protocols were used for preparation of different sample solution sets.

Protocol I. For SAXS, long DNA in pure water, and concentration range 3−130 g/L. A mother solution of 130 g/L was prepared by adding 13.0 mg of dry DNA fibers and 100 μL pure water into a polyethylene bag (20 μm thick film). The bag was then inserted into the sample holder of the SAXS instrument for measurements. Lower concentrations were prepared by diluting the same sample (in the original bag) with water. The higher concentration solutions are rather viscous, and manipulation in the bag facilitated sample homogenization, without excessive mixing or vortexing that would shear the chains.

Protocol II. For SAXS, HA in pure water, and concentration range 10−100 g/L. The set of solutions was prepared by dissolving weighted amounts of dry HA grains in adequate amounts of pure water, and equilibration at 4 °C for a week. They were mixed with a pipet or a spatula before application to SAXS sample holder.

Protocol III. For FCS measurements of the diffusion coefficient of DNA fragments.[19] Fluorescently labeled DNA 110bp fragments (DNA110*) with Cy5 fluorophore at one end were obtained from Microsynth AG. In order to achieve a 20 nM fluorophore concentration, required for FCS, we added 2 μL of a DNA110* stock solution (500 μM in basepairs) into 500 μL aliquots of long DNA, HA or DNA146 samples of varying concentrations (DNA: 0.0015−22.5 mM or 0.001−15 g/L, HA: 0.0025−5 mM or 0.001−2 g/L). These were prepared either in 10 mM TE (Tris-Cl pH7.5 +1 mM EDTA) buffer or in pure water, where only traces of the buffer <0.05 mM were present, originating from the addition of labeled DNA stock.

Small-Angle X-ray Scattering. Small angle X-ray scattering experiments were performed on two Kratky cameras which were equipped with linear position sensitive detectors (PSD 50, Hecus X-ray system) and sealed tube generators with copper anode. Cu Kα radiation (λ = 1.542 Å) was selected with Ni filter in combination with a pulse height discriminator.

SAXS intensity curves from DNA solutions were acquired by using the camera mounted on 1 kW tube while beam size was set to 0.2 mm ×3 mm. The path between the sample and the detector (=50 cm) was evacuated to reduce background scattering. DNA solution was enclosed into a polyethylene bag (see protocol I above) while pure water in such a bag was used for background measurements.

For HA experiments we used a System 3 camera (Hecus X-ray Systems, Graz, Austria) with a beam size of 0.5 mm ×3.5 mm, sample−detector distance of 30 cm and a 2 kW tube. Thus, more intense primary beam was used for HA samples and, as a whole camera is evacuated, the air scattering (background) is lower which is particularly important for weakly scattering samples like HA. A small amount of the HA solutions was applied in the sample holder of the SAXS instrument by a pipet or, for higher concentrations, a spatula was used. Then, the sample was enclosed by mylar windows. For all samples, experiments were performed at room temperature with exposure times of 900 s. The scattering from the pure water was subtracted from the data and thus only scattering intensity contributions from the macromolecules and counterions was analyzed.

SAXS data were reported as a function of q, the magnitude of the scattering vector, defined by the angle between the incidence and scattered radiation 2θ and the X-ray wavelength λ through the relation $q = (4\pi/\lambda)\sin(\theta)$. The angular calibration was performed with silver-stearate and silver-behenate standards. Using the above configurations, the accessible ranges of the scattering vector q were 0.1−3.1 nm^{-1} and 0.09−5.5 nm^{-1} for DNA and HA experiments, respectively.

Fluorescence Correlation Spectroscopy. We have used Zeiss ConfoCor II FCS instrument. The focal volume was defined by a Zeiss Plan-NeoFluar 100x/NA1.3 water immersion objective, epi-illumination was by He−Ne 632.8 nm 5 mW laser, for excitation of the Cy5 fluorophore. Measurements were performed at 25 °C, the ambient temperature of the temperature stabilized clean-room.

Fluorescence correlation spectroscopy is used to measure the diffusion coefficient of the fluorescently labeled molecules. Number fluctuations of the molecules entering and leaving the focal volume of the instrument are registered as fluorescence variation. An autocorrelation function is calculated for the fluorescence intensity trace. In other words, the signal is analyzed for self-similarity after the lag time τ:

$$G(\tau) = 1 + \frac{1}{N_f}\frac{1}{1+\frac{\tau}{\tau_D}}\frac{1}{\sqrt{\left(1+\left(\frac{w_0}{z_0}\right)^2\frac{\tau}{\tau_D}\right)}}\left(1+\frac{T}{1-T}\exp\left(-\frac{\tau}{\tau_T}\right)\right) \quad (2)$$

Here, N_f is the average number of fluorescent molecules in the focal volume, z_0/w_0 is the focal volume structure parameter and T, average fraction of fluorophores in the triplet state (thus, nonfluorescing). The lifetime τ_T of the triplet state is taken into account when fitting. The characteristic decay time τ_D is the diffusion time that the fluorescent molecule takes to traverse the focal volume. The details of the procedure we used to extract τ_D may be found in.[19] For demonstration, in Figure 2, besides the $G(\tau)$ experimental curve and

dx.doi.org/10.1021/ma3021486 | Macromolecules 2013, 46, 1107−1118

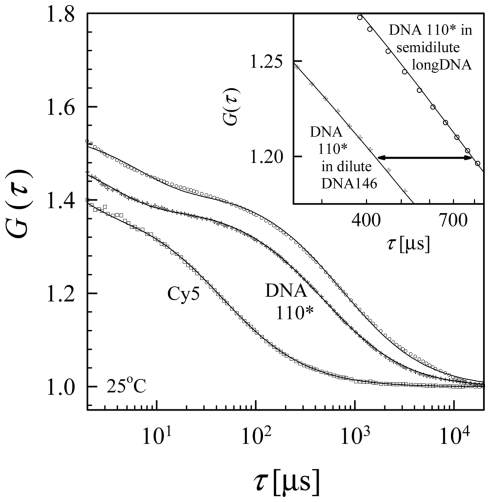

Figure 2. Experimental autocorrelation functions $G(\tau)$ recorded for fluorescently labeled 110 bp double-stranded DNA fragments: DNA110* in semidilute long DNA solution or in dilute DNA146 solution (2 μM DNA110* in 0.2 mM, either long DNA or DNA146 in very low salt conditions <0.05 mM). For comparison, the autocorrelation function (denoted Cy5) is shown for 20 nM Cy5 fluorophore in pure water, without any DNA. The inset zooms the correlation time range 250−850 μs. The arrow in the inset denotes 350 μs difference between the respective diffusion times obtained by fits. The experimental values of $G(\tau)$ are shown with symbols and the respective fits with lines.

fit for Cy5 (as a standard), we present the $G(\tau)$ curves recorded for DNA110* in semidilute long DNA solution or in dilute DNA146 solution (2 μM DNA110* in 0.2 mM long DNA or DNA146 in very low salt <0.05 mM). The inset emphasizes the difference between the diffusion times and how well the experimental data may be fitted.

The diffusion time, extracted by fits to eq 2 is inversely proportional to the self-diffusion coefficient D. The relationship between τ_D and D may be obtained from the measurement of τ_{Cy5} for Cy5 fluorophore itself, whose diffusion coefficient is known, $D_{Cy5} = 3.16 \times 10^{-10}$ m^2/s:[40]

$$D = D_{Cy5}\frac{\tau_{Cy5}}{\tau_D} \quad (3)$$

The diffusion coefficients D that we obtain from τ_D are for the fluorescently labeled DNA110* molecules, diffusing in solutions that contain varying concentrations of HA, long DNA or DNA146. That is, we obtain D^{exp}_{110*}, diffusion coefficient for DNA110* which, however, depends on monomer concentration c of these solutions. We remind that the double stranded DNA (dsDNA) persistence length L_p = 50 nm[31] is comparable to the contour length of DNA110*, 38 nm. Therefore, we expect that DNA110* assumes an extended, rodlike configuration. According to Tirado et al.[41] the translational diffusion coefficient calculated for a rodlike macromolecule is given by

$$D^{th} = \frac{kT}{3\pi\eta}\frac{\ln(L_c/d) + 0.312}{L_c} \quad (4)$$

Here $L_c = Nb$ is contour length, d is polyion diameter, $\eta = 8.9 \times 10^{-4}$ Pas is viscosity of water (T = 298 K). With b = 0.34 nm and d = 2.6 nm, the diffusion coefficient for 110bp DNA is $D^{th}_{110*} = 3.98 \times 10^{-11}$ m^2/s. Stellwagen et al.[42] have reviewed the literature and shown that the expression by Tirado et al. is well applicable to experimental data obtained for DNA molecules in size from 10 to 1000 basepairs.

RESULTS

SAXS. The scattering curves for long DNA and HA solutions at different concentrations are presented in Figure 3 and 4, respectively. The scattering intensities obtained for both systems as a function of q may be roughly subdivided into three regions. Below 0.2 nm^{-1} there is the typical polyelectrolyte upturn. This feature has been observed, studied and discussed by others[15,22,37,43] and was related to formation of chain aggregates or locally ordered domains. At the highest q-values, all curves decrease roughly as q^{-1}. This scattering intensity dependence is typical of rodlike scatterers, and the segments of polyelectrolyte chains may easily be taken as such.[23,37,44] In an intermediate q-range, which we examine further in more details, intensity curves reveal characteristic features which reflect the structure of the solution.

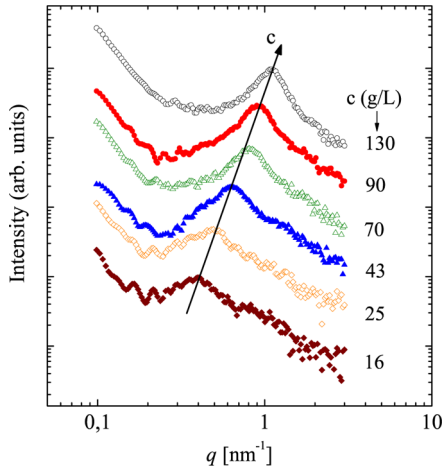

Figure 3. SAXS intensity vs scattering wave vector q at T = 25 °C for pure water DNA solutions (concentrations 16−130 g/L). The arrow denotes the shift with concentration of the position of the peak, corresponding to a wave vector q_m. The curves have been shifted for clarity.

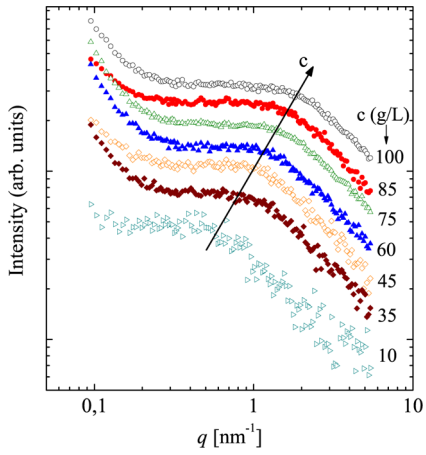

Figure 4. SAXS intensity vs scattering wave vector q at T = 25 °C for pure water HA solutions (concentrations 10−100 g/L). The arrow denotes the shift with concentration of the position of the shoulder, corresponding to a wave vector q_m. The curves have been shifted for clarity.

The intensity curves for long DNA (Figure 3) display a broad maximum often called the polyelectrolyte scattering peak. The position of the maximum, q_m, shifts toward higher wave vectors and greater intensity with increasing DNA concentration. Such a behavior is common for polyelectrolyte solutions at low added salt conditions.[22,45,46] We also note that

dx.doi.org/10.1021/ma3021486 | Macromolecules 2013, 46, 1107−1118

we obtained similar q_m values for our solutions of micrometer-sized, polydisperse DNA as did Bloomfield and Wang[25] for solutions of monodisperse, rod-like nucleosomal DNA fragments only 50 nm long. This is a precise demonstration (after Koch et al.[15]) of the fact that in a semidilute solution identity of polyion segments is lost—it is not possible to discern whether a segment found in the vicinity of another is part of the same chain or another one. In other words, the solution structure, the arrangement of all the segments connected in chains, i.e., long DNA, appears similar to the arrangement of separate segments, i.e., rod-like short DNA molecules.

Our data for pure water solutions of HA are shown in Figure 4. The marked difference between DNA and HA sets of data is immediately obvious: A well pronounced correlation peak is missing in the scattering intensities measured for HA solutions, only a shoulder appears. However, it is clear from Figure 4 that the shoulder shifts toward higher q with increasing concentration, indicating changes in the local structure of the HA mesh. Only Villetti et al.,[37] to the best of our knowledge, reported SAXS of HA solution (15 g/L) from our HA concentration range. Notably, their scattering curve features also a shoulder at a q-position that fits into our data set. Moreover, they noticed that the absence of the polyelectrolyte peak can be attributed to the weak electrostatic nature of HA chains and, upon shearing, the electrostatic interaction is magnified and the polyelectrolyte peak was restored at the place of the shoulder. This is in accordance with the calculated scattering intensity as a function of the interaction strength between the polyelectrolyte segments.[23,24] Further interpretation of HA scattering intensities may be found in Supporting Information.

Following the above, in order for us to be able to compare the results for HA and DNA, we attempt to determine q_m from the HA spectra in a simple, model-independent way. We propose that the shoulder position in HA scattering curves could be regarded as the polyelectrolyte peak position q_m. As any choice would be rather arbitrary and also to simplify the analysis, q_m is taken to be at the intersection of the q^{-1} line and the q independent part of the curve, as presented for 85 g/L HA solution, Figure 5.

With this choice of q_m for HA, in Figure 6 we present the evolution of q_m as a function of either DNA or HA concentration. Data by Bloomfield and Wang[25] for solutions of monodisperse DNA fragments is shown for comparison. Indeed, as expected for semidilute solutions, q_m scales with concentration as $c^{1/2}$ for both HA and DNA.[14,20,25]

FCS. In Figure 7 we present D^{exp}_{110*}, the diffusion coefficient of DNA110* polyion in various conditions. In the upper panel we present the homogeneous system DNA110*/DNA146, where the labeled DNA110* polyions diffuse in the environment of similarly sized DNA146 fragments. In the lower panel we show data for the hetereogeneous systems DNA110*/DNA and DNA110*/HA, where the labeled DNA110* polyions diffuse in the mesh formed by long DNA or HA chains. The values of D^{exp}_{110*} are shown as a function of the monomer concentration c of the polyelectrolyte that defines the system in question. The concentration range of the FCS study overlaps with the range of the correlation length/mesh size studies by SAXS and DS.[18,33]

Homogeneous System DNA110/DNA146.* First, we address the behavior of the homogeneous system DNA110*/DNA146 in 10 mM TE buffer (Figure 7, upper panel). Below c = 1−2 mM, D^{exp}_{110*}(DNA146) is constant within the

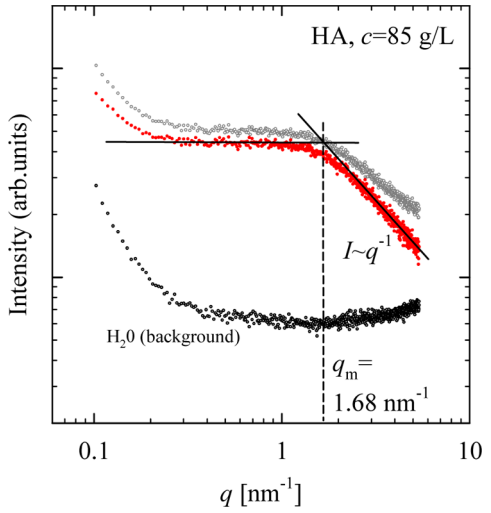

Figure 5. SAXS intensity for HA solution 85 g/L (topmost curve). This data is subtracted for the background (H_2O) intensity. The resulting intensity curve features q^{-1} dependence at high q. The shoulder position, q_m is taken to be at the intersection of the q^{-1} line and the horizontal line.

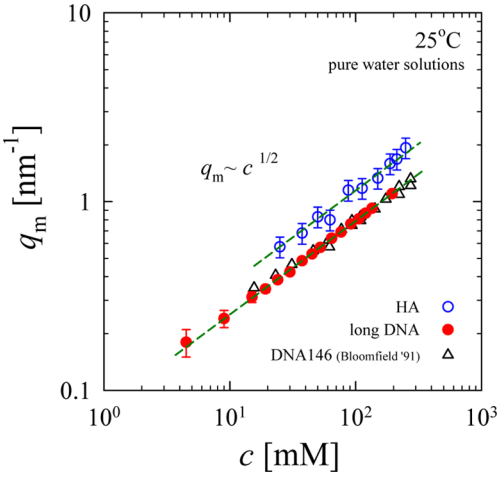

Figure 6. Characteristic wave-vector q_m extracted from the scattering curves for pure water long DNA and HA solutions is shown versus polyelectrolyte monomer concentration. We note that we obtained similar q_m values for solutions of μm-long, polydisperse DNA as Bloomfield and Wang[25] obtained for solutions of monodisperse 50 nm nucleosomal DNA fragments. The dashed lines denote that q_m scales with the square root of the concentration both for HA and DNA.

experimental error, with the average value D^{exp}_{110*}(DNA146) = 3.9 ± 0.1 × 10^{-11} m^2/s. This value is very close to the theoretical value D^{th}_{110*} of the self-diffusion coefficient for rodlike particles, eq 4 (see Experimental Methods, FCS section). It is also very close to the value 3.95 × 10^{-11} m^2/s that we obtained for DNA110* diluted down to 1.5 μM directly with 10 mM TE buffer (without DNA146).

The decrease of D^{exp}_{110*}(DNA146) above c = 1−2 mM is due to the excluded volume effects and relates well with the dilute-semidilute crossover concentration for 40−50 nm long rodlike DNA molecules[25,34] that we work with. The self-diffusion coefficient has been previously shown to decrease linearly with the volume fraction Φ of rod-like particles, for e.g. a mineral, boehmite, L≈300 nm,[47] and 20 bp dsDNA L≈7 nm:[48]

dx.doi.org/10.1021/ma3021486 | Macromolecules 2013, 46, 1107−1118

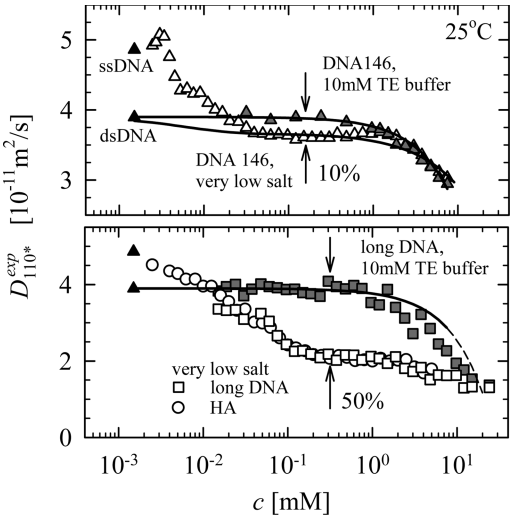

Figure 7. Diffusion coefficient D^{exp}_{110*} for 1.5−2 μM DNA110* diffusing in various conditions/solutions. Upper panel: DNA110* in DNA146 in very low salt <0.05 mM conditions (open triangles) or in DNA146 in 10 mM TE buffer (shaded triangles). Lower panel: DNA110* in long DNA solutions (open squares) or HA solutions (open circles) in very low salt <0.05 mM conditions, as well as in long DNA in 10 mM TE buffer (shaded squares). Both panels: The values at 1.5 μM (black triangles) stand for a 110 bases long single stranded DNA oligomer (ssDNA) diluted directly with pure water and for a 110bp double stranded DNA110* (dsDNA) diluted directly with 10 mM TE buffer. The arrows denote the reduction of D^{exp}_{110*} between the buffer and very low salt solutions (10% for DNA110* in DNA146 and 50% for DNA110* in long DNA). The full lines denote fits of eq 5 to D^{exp}_{110*} values for DNA110*/DNA146 in buffer and in very low salt conditions. The fit for DNA110*/DNA146 in the buffer is reproduced in the lower panel and is also extrapolated to higher concentrations (dashed line).

$$D(c) = D_0(1 - \alpha\Phi) \tag{5}$$

Here, D_0 would be the self-diffusion coefficient measured in infinitely dilute solution. As stated above, our experimental values at practically infinite dilution of 1.5 μM are very close to the theoretical D^{th}_{110*}, thus the latter we take as D_0. For DNA, molar concentration c (in mM) is related to volume fraction as $\Phi \approx 0.001c$. The slope α depends on the aspect ratio $p = L_c/d$ of the particle (polyion), according to the variational calculation by Dhont et al.:[47]

$$\alpha = 2 + \frac{10}{32}(p - 1) + \frac{1}{53}(p - 1)^2 \tag{6}$$

For DNA110*, $p \approx 15$, leads to $\alpha \approx 10-15$. Fit of eq 5 to D^{exp}_{110*}(DNA146) gives $\alpha \approx 30$ (full line in Figure 7, upper panel), in a reasonable agreement with the theoretical value. Wilk et al.[48] observed a similar difference between the theoretical and experimental slope, and attributed this difference to a contribution of the counterion atmosphere to the volume fraction.

Second, we address the behavior of the homogeneous system DNA110*/DNA146 in very low salt conditions (Figure 7, upper panel). A principal feature is that in the concentration range 0.02−1 mM, D^{exp}_{110*}(DNA146) in very low salt conditions appears reduced for about 10% compared to values in buffer. This reduction of the diffusion coefficient with reduction in the ionic strength is also the effect of the counterion atmosphere on the volume occupied by DNA fragments. In order to check this concept by Wilk et al. we recalculated the fragment volume in order to fit eq 5 also to our very low salt data set.

That is, for the diameter of the DNA fragments we took $d + \kappa^{-1}/k$ and for the length $L_c + \kappa^{-1}/k$, where k is an arbitrary factor and κ^{-1} is the Debye screening length, defined by the counterion concentration in the absence of added salt (see Appendix A). We used a following expression for the Debye length dependence on DNA dmonomer concentration c:

$$\kappa^{-1} \propto \left(z_m \frac{c}{\eta} + c_s\right)^{-1/2} \tag{7}$$

Here, $z_m = 2$ accounts for the two charges a DNA monomer carries and $\eta = 4.2$ is the Manning condensation factor—only the uncondensed charges form the counterion atmosphere. We also introduced a residual level of salt, $c_s = 0.01$ mM. This is due to labeled DNA110* buffer traces in the solutions of DNA146 that we studied and also due to CO_2 dissolved in pure water.

Thus, the volume fraction $\Phi \approx 0.001c$ becomes enhanced by a factor (which is dependent on the DNA concentration due to κ^{-1} dependence):

$$\Phi_{eff} = 0.001c\frac{(L_c + \kappa^{-1}/k)(d + \kappa^{-1}/k)^2}{L_c d^2} \tag{8}$$

Furthermore, we note that the slope $\alpha(c)$ is a function of the DNA fragment aspect ratio p, which now depends on DNA concentration c due to κ^{-1} dependence

$$p_{\text{eff}} = (L_c + \kappa^{-1}/k)/(d + \kappa^{-1}/k) \tag{9}$$

Combining eqs 6−9 into eq 5, we get an expression where the only free parameter is k. The best fit of thus corrected eq 5 to our very low salt data set we get for $k = 1.5$, see Figure 7. Wilk et al. also found k is between 1 and 2. Thus, we successfully reproduce the 10% reduction for D^{exp}_{110*}(DNA146) in very low salt conditions compared to values in buffer. For a shorter, 20 bp fragment that Wilk et al. studied, the enhanced volume is relatively large (it depends on κ^{-1}/L_c), thus they observed a stronger reduction of the diffusion coefficient of 20−25%, also reproduced by their fits. The fits of eq 5 to both D^{exp}_{110*}(DNA146) in very low salt conditions and in buffer merge above c = 1−2 mM (as well as the experimental data), indicating that the volume enhancement due to κ^{-1} becomes negligible.

Another important feature of D^{exp}_{110*}(DNA146) in very low salt conditions is that below c = 0.02 mM it increases above D^{th}_{110*}. We ascribe this to denaturation of the DNA110* probe. Naturally, DNA146 should also denature there, but DNA146 concentration is so low that it has no influence on DNA110* diffusion. At these very low concentrations DNA dissolved in pure water denatures, as the unscreened Coulomb repulsion of phosphate groups tears the strands apart.[49] Presumably, below c = 0.02 mM we are measuring the diffusion of a mixture of single stranded and double stranded DNA110*, where single stranded DNA (ssDNA) proportion increases as the solution gets diluted. The notion that our DNA110*/DNA146 solution denatures gradually upon dilution with pure water is primarily supported by the following. The D^{exp}_{110*} at the lowest concentrations reaches the value for a ssDNA oligomer 110 bases long, dissolved directly in pure water, without DNA 146. This ssDNA value may also be compared to the values obtained by Tinland et al. for diffusion coefficients of ssDNA fragments from 280 to 5386 bases long.[50]

dx.doi.org/10.1021/ma3021486 | Macromolecules 2013, 46, 1107−1118

Heterogeneous Systems DNA110/HA and DNA110*/DNA.* Notably, the heterogeneous systems, DNA110*/HA and DNA110*/DNA, show similar behavior, both quantitatively and qualitatively (Figure 7, lower panel). Both these also present analogueies with the homogeneous system.

First, we note that below c = 1−2 mM D_{110*}^{exp}(longDNA) in 10 mM TE buffer is similar to the values for the homogeneous system in buffer. This experimental value is similar to the theoretical one, D_{110*}^{th} for a freely diffusing 110 bp DNA fragment, see eq 4. In other words, D_{110*}^{exp} in buffer is independent of the *matrix* (dilute DNA146 fragments or semidilute polydisperse long DNA) below c = 1−2 mM. There the probe DNA110* diffuses freely.

Second analogy is that the decrease of the diffusion coefficient toward higher concentrations starts for DNA110*/HA and DNA110*/DNA above c = 1−2 mM just as for DNA110*/DNA146, both in low salt and buffered solutions, indicating the effect of the increase in the volume fraction. For a given concentration the volume fraction should be quite similar between the DNA146, long DNA, and HA systems. Structurally, all the systems may be considered similar (see Figure 6), since DNA146 is in the semidilute regime above c = 1−2 mM, as well as HA and long DNA. The varied magnitudes of D_{110*}^{exp} decrease demonstrate different dynamics of the homogeneous and heterogeneous systems. Eventually, if we extend the fit for the homogeneous system (dashed line in Figure 7, lower panel), it will reach similar diffusion coefficient values as for the heterogeneous system about 20−30 mM. At these concentrations, also the difference dissappears between very low salt and buffered environments for the heterogeneous, as well as for the homogeneous system.

Third analogy is that for the heterogeneous DNA110*/DNA system, as for the homogeneous DNA110*/DNA146 system, there is an intermediate concentration region where D_{110*}^{exp} in very low salt conditions is reduced in comparison to D_{110*}^{exp} in buffer (see Discussion).

In a final analogy, D_{110*}^{exp} for the heterogeneous system DNA110*/HA, below c = 0.02 mM, in very low salt conditions, increases above the theoretical value D_{110*}^{th} and reaches the values similar as those for the homogeneous system DNA110*/DNA146 and also the value for ssDNA 110 bases long. Again, as for the homogeneous system, we ascribe this increase in D_{110*}^{exp} to the DNA denaturation. Notably, denaturation of DNA110* starts in HA solution as well as in DNA146 solution below a rather similar monomer and/or counterion concentration. This indicates that the probe DNA110* stability depends only on the ionic strength of the solution, defined by the counterions coming of the polyions, whether DNA or HA. In brief, diluting either DNA or HA reduces the counterion concentration, thus reduces the screening (κ^{-1} reaches 80−100 nm, see Figure 8) and leads to DNA110* denaturation and the consequent increase of D_{110*}^{exp}.

DISCUSSION

Mesh Size. In the Introduction we emphasized that for a polyelectrolyte that appears as highly stretched polyions (rods) the least dense way of packing is an isotropic mesh of rods that is characterized by a mesh size $(bn)^{-1/2}$. Here n is the number concentration of monomers and b is the monomer size of the polyelectrolyte in question. In other words, the mesh size for a rigid polyelectrolyte is simply defined by the total contour length of all the polyions in the solution. However, if the polyion is not so rigid and not all the monomers are charged it

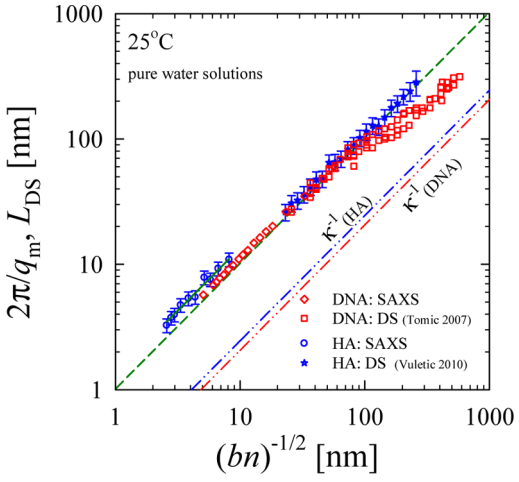

Figure 8. Correlation length $\xi = 2\pi/q_m$ calculated from the characteristic wave-vector q_m in SAXS intensity and the length scale L_{DS}, obtained by dielectric spectroscopy[18,33] (we considered the MHz range relaxation). These techniques cover complementary concentration ranges of semidilute DNA and HA solutions. Length scales are shown vs native length scale of the polyelectrolyte, mesh size $(bn)^{-1/2}$. Here, n is the number concentration of monomers and b is the monomer size, for DNA b = 0.34 nm and for HA b = 1 nm. For comparison we also show Debye lengths calculated (see Appendix A) for DNA and for HA.

may coil.[8] Locally, several monomers carrying a small number of charges would form electrostatic blobs which then carry enough charge to repel each other. The polyion then appears as a rigid chain of such blobs. Effective length of such a chain would be shorter than the original polyion contour length—the monomer size would be reduced for a factor:

$$B = (A^2/u)^{2/7} \tag{10}$$

where A is the number of monomers between the charges and the parameter $u = l_B/b$, a ratio of the Bjerrum length (see Appendix A) and the monomer size. Accordingly, the mesh size would increase to $(bn/B)^{-1/2}$. The validity of this concept has been demonstrated for various flexible, synthetic polyelectrolytes by Combet et al.[28] That is, these authors established that the correlation length $\xi = 2\pi/q_m$ as experimentally obtained by SAXS is equal to the polyelectrolyte concentration dependent mesh cell size given by $(bn/B)^{-1/2}$.

We may consider this concept also for semirigid polyelectrolytes like DNA and HA. However, in the following we show that the theoretically presumed reduction in the chain length is quite small and also that one electrostatic blob consists of about one monomer of DNA or HA, which renders the concept irrelevant. HA has one charge per monomer (z_m = 1; z_m is the number of charges on the monomer) of the length b_{HA} = 1 nm,[27,51] which is longer than the Bjerrum length l_B = 0.72 nm. Thus, the Manning charge density parameter $\eta = z_m u$ = 0.7 for HA is smaller than 1 and its counterions do not Manning condense.[6,7] Thus, for HA, the factor A equals one. Consequently, eq 10 gives for HA B = 1.1. For DNA, there are two charges per monomer (z_m = 2) and b_{DNA} = 0.34 nm which gives η = 4.2. Accordingly, about 3 out of 4 counterions are condensed. In other words, only 1 out of 4 charges on DNA remains uncompensated and we get A = 2, while u = 2. Thus, for DNA eq 10 gives B = 1.2. Here we note that these corrections to the mesh size would be 5−10% and could be almost within the experimental error. Furthermore, the size of

dx.doi.org/10.1021/ma3021486 | *Macromolecules* 2013, 46, 1107−1118

putative electrostatic blobs in this model is $S = bB^{3/2} \sim b$. In other words, the model has a trivial solution—a single monomer as the electrostatic blob. Also, as DNA and HA structural persistence length is much larger than the monomer size, their polyion chains are certainly extended on the length scale of the electrostatic blob.

Indeed, in Figure 8 we show that for DNA the correlation lengths $\xi = 2\pi/q_m$, as experimentally obtained by SAXS, are practically equal to the polyelectrolyte concentration dependent mesh cell sizes given by $(bn)^{-1/2}$. For HA, experimental values $\xi = 2\pi/q_m$ are close to the $1.2\cdot(bn)^{-1/2}$ line. We get this despite the fact that HA lacks the SAXS peak routinely obtained for other, highly charged polyelectrolytes. This strongly supports our proposition that the shoulder represents the equivalent of the polyelectrolyte peak for the weak polyelectrolyte HA. Presumably some systematic error, specific for the methodology used in extracting q_m from the HA shoulder, caused the correlation lengths to be consistently high by a factor of 1.2.

We also note that in the concentration range studied by SAXS the mesh sizes are smaller than the structural persistence lengths of HA or DNA and that the depiction of the solution as an isotropic mesh of rods may well apply.

The local structure of the polyelectrolyte mesh can not be studied by SAXS at concentrations below about 3 g/L, as the scattering peak becomes weak and overlaps with the steep intensity upturn at low q. At these low concentrations the mesh size would be significantly larger than the structural persistence length of the semirigid polyions. A question is whether the polyions may form there an isotropic mesh of rods, i.e., whether the electrostatic contribution to the persistence length may be sufficient to keep the polyions and the mesh they form rigid.[27,32,52]

Our previous studies by dielectric spectroscopy (DS)[18,33] in this lower concentration range have provided a length scale, l that scales as a correlation length, that is $l \propto c^{-1/2}$ both for long DNA and HA. If we rescale l obtained either for long DNA or HA for a same factor (2π) and plot it against the mesh size, we get that $2\pi l = L_{DS} = (bn)^{-1/2}$. That is, L_{DS} length scale for either DNA or HA falls at the same master line, as does the $\xi = 2\pi/q_m$ length scale obtained by SAXS, Figure 8. Here we note that κ^{-1}, the Debye screening length which is defined only by the counterions (see Appendix A) released from polyions would also scale in the same manner. Indeed, κ^{-1} is rather close in absolute value to l: $\kappa^{-1} = (1/4.5)(bn)^{-1/2}$ and $l = (1/2\pi)(bn)^{-1/2}$. However, our DS studies showed that l does not change upon addition of salt to initially salt free solutions. This strongly indicated that l is not a screening length in nature. Furthermore, this length scale was observed by DS also for a dilute solution of DNA146 fragments where it scaled as $l \propto c^{-1/3}$—as the average distance between chains (see Supporting Information).[34] Thus, $L_{DS} = 2\pi l$ was identified as a property of an ensemble of chains—which is a correlation length and not a screening length. Additional analysis regarding the deviation of L_{DS} from $(bn)^{-1/2}$ line for DNA at low concentrations is given in the Supporting Information.

To summarize, two complementary studies, the dynamics study and a more conventional structural study of two semirigid polyelectrolytes, DNA and HA, across 4 orders of magnitude in concentration, have provided a single length scale. This length scale spans the range from 3 to 600 nm and equals the mesh size $(bn)^{-1/2}$ of an isotropic mesh of rods. In other words, HA and DNA in very low salt conditions may be consistently regarded as an isotropic mesh of rodlike polyions, across the semidilute concentration range 0.01−100 g/L.

Probing the Mesh. We probed this mesh by observing the diffusion of a 110 bp DNA fragment with $L_c \approx 40$ nm. Such a rodlike fragment of an intermediate size provided the opportunity to probe a tight mesh (mesh sizes smaller than the fragment) and open mesh (mesh sizes larger than the fragment). In Figure 9 we present the experimentally obtained

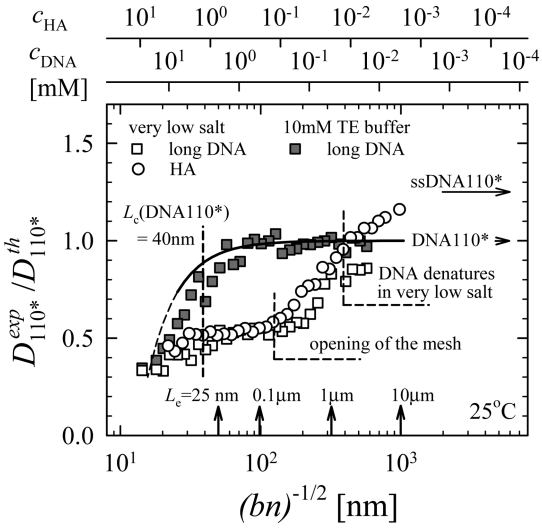

Figure 9. Diffusion coefficient D^{exp}_{110*} for 1.5−2 μM DNA110* diffusing in various conditions/solutions, normalized to the theoretical value D^{th}_{110*} and shown vs native length scale of the polyelectrolyte, mesh size $(bn)^{-1/2}$. Data are for DNA110* in long DNA solutions (shaded squares) in 10 mM TE buffer and for DNA110* in long DNA (open squares) or HA solutions (open circles) in very low salt <0.05 mM conditions. The full line denotes theoretical values for a monodisperse solution of DNA110*—based on a fit of eq 5 to D^{exp}_{110*} values for DNA110*/DNA146 in buffer (see Figure 7). The fit is extrapolated to higher concentrations, i.e. smaller mesh sizes (dashed line). At low concentrations the experimental values and the fit are equal to D^{th}_{110*}, thus DNA110* label and an arrow denote the value of 1. The value for a 110 bases long single stranded DNA oligomer (ssDNA110*) diluted directly with pure water is also denoted. Several values of L_e, the electrostatic contribution (OSF model) to the persistence length are denoted. There is a correspondence (arrows) of L_e and $(bn)^{-1/2}$ as both depend on the monomer concentration.

diffusion coefficients D^{exp}_{110*} for DNA110* either in HA or long DNA, normalized to the theoretical self-diffusion value at infinite dilution. This ratio is then presented vs native length scale of the studied polyelectrolytes, mesh size $(bn)^{-1/2}$. We also present a fit to D^{exp}_{110*} measured for the probe DNA110* in DNA146 solution (in 10 mM buffer). The fit is to the occupied volume model that explains rather well the concentration dependence of the diffusion coefficient for the rodlike, charged particles (see also Figure 7).[47,48] We remind that DNA110*/DNA146 solution is practically monodiperse and is dilute below 1−2 mM and thus there the mesh size is not defined (although the correlation length is—see Supporting Infromation). However, we simply transformed the monomer concentration c of DNA110*/DNA146 into a number concentration n and calculated the corresponding $(bn)^{-1/2}$ values. We take this as a reference for the behavior of D^{exp}_{110*} in the mesh formed by long DNA or HA. In Figure 9 we also show D^{exp}_{110*} values for the probe DNA110* without any *matrix*, either DNA146, HA or long DNA. The values are given for the

dx.doi.org/10.1021/ma3021486 | Macromolecules 2013, 46, 1107−1118

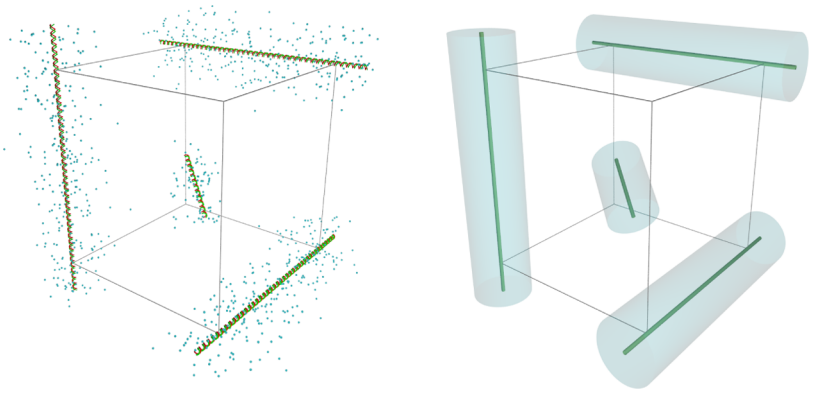

Figure 10. Polyelectrolyte mesh formed by DNA, mesh size $(bn)^{-1/2} \approx 100-150$ nm at 0.3 mM (in base pairs). In the very low salt conditions, for the mesh to open completely, i.e., the DNA fragment to reach the free diffusion coefficient values, the mesh size (edge of the cube) needs to become even larger (300−400 nm compared to the fragment length $L_c \approx 40$ nm). In a solution of finite ionic strength the mesh opens immediately when the mesh size becomes larger than the fragment length. The thickness of the counterion atmosphere is comparable to the Debye length κ^{-1} and defines the enhanced occupied volume (shaded cylinders) of the polyions. In the very low salt conditions κ^{-1} is defined only by the counterions (small spheres) and scales with the mesh size but it is quite smaller, $\kappa^{-1} \approx (1/5)(bn)^{-1/2}$.

probe in double stranded (DNA110*) as well as in the single stranded form (ssDNA110*).

First, we address the properties of the mesh in the finite ionic strength conditions, where we studied only DNA110*/long DNA heterogeneous system. When the mesh size formed by the long, polydisperse DNA chains is larger than the contour length ($L_c \approx 40$ nm) of the probe DNA110 fragment, the probe diffuses freely—D^{exp}_{110*} is similar, within the experimental error to the theoretical self-diffusion coefficient value, as well as to the experimental one obtained for DNA110* at very high dilution. D^{exp}_{110*}(long DNA) is independent of the mesh size, from 50 to 60 nm up to 600 nm (corresponds to 1−0.01 mM DNA monomer concentration). In analogy to the homogeneous DNA110*/DNA146 system, the ionic strength of 10 mM TE buffer is sufficient to reduce the Debye length and the thickness of the counterion atmosphere to the levels where the atmosphere does not contribute significantly to the occupied volume—thus there is no reduction in D^{exp}_{110*} below D^{th}_{110*}. On the other hand, when the mesh size becomes comparable to DNA110* size, we observe a decrease of D^{exp}_{110*}(long DNA), presumably due to the occupied volume effects, as for the DNA110*/DNA146 system. The occupied volume should be similar between the long polydisperse DNA and DNA146, as the counterion concentrations and thus the counterion atmosphere thickness is the same. However, D^{exp}_{110*} decrease occurs more steeply in DNA110*/long DNA than for DNA110*/DNA146. Also, structurally, both systems are similar there—DNA146 solution (matrix of DNA110*/DNA146 system) is semidilute when the correlation length/mesh size is smaller than its contour length, 50 nm and the scattering experiments do not distinguish the two semidilute systems (see Figure 6). We may speculate here on influence of the mesh formed by the long DNA molecules. The rigid mesh—here the mesh size becomes smaller than the structural persistence length of DNA—could present an additional obstacle for the probe DNA. We will elaborate on this influence further below. Eventually, for the mesh size of 15−20 nm, all data sets appear to converge, as well as the extrapolation of DNA110*/DNA146 fit. Presumably, the occupied volume effects dominate here and this regime may be understood as the crowded environment.[29,30]

Second, we argue that our data show that, in semidilute solution, the polyions in very low salt conditions may form a rigid mesh that presents an additional obstacle to probe molecule diffusion. This effect is in addition to the effect of the polyion chain occupied volume enhancement due to counterion atmosphere expansion in very low salt conditions. The latter effect explains quite well the diffusion coefficient of our probe DNA110* in the *matrix* of monodisperse DNA146 both in very low salt conditions and in buffer. For the semidilute polydisperse *matrix* of DNA or HA we observed a significant, 50% reduction of D^{exp}_{110*} in very low salt in comparison to D^{exp}_{110*} in buffer, while the enhanced volume occupied by the polyions may account for only 10% of this reduction, as we have seen for the homogeneous DNA110*/DNA146 system. Also, in very low salt conditions the mesh has to be about 3 times larger than the probe length (Figure 10) in order for D^{exp}_{110*} only to start to rise toward D^{th}_{110*}. Eventually, in a very open, 400 nm mesh DNA110* is able to diffuse freely in very low salt conditions. On the contrary, when in buffer, DNA110* is able to diffuse freely already in 60 nm mesh—this mesh size is just slightly larger than the probe (40 nm).

We remind that the mesh size is fundamentally a geometrical property of a solution of a given concetration—it does not tell on the e.g. flexibility of polyions. An interesting issue is how the structure and dynamics of the mesh formed by the polymer change with the persistence length of the chains. Polyelectrolytes with their electrostatics dependent persistence length present an interesting case. In the very low salt conditions the Debye length and thus the electrostatic contribution to the persistence length, L_e (OSF model, see Appendix A) are controlled by the counterion concentration.

Henceforth, for a given monomer concentration c and the related mesh size $(bn)^{-1/2}$ one may calculate a Debye length κ^{-1} and the corresponding $L_e \propto \kappa^{-2}$ value. The values L_e are denoted vs mesh size in Figure 9. Already Hayter et al.[44] discussed that the electrostatic persistence length defined only by counterions in the salt free conditions would be dominant over the persistence length defined by the random collisions between one chain and its neigbours. Experimentally, the electrostatic contribution L_e was studied both for DNA and HA.[27,31,53] From these works, it is apparent that for DNA and HA solutions in very low salt conditions the total persistence

dx.doi.org/10.1021/ma3021486 | *Macromolecules* 2013, 46, 1107−1118

length would be comparable or larger than the mesh size across the studied concentration range. On the other hand, 10 mM buffer is quite enough to reduce the persistence length to its structural value[27,31,53]—for our DNA and HA systems in the buffer the persistence length is smaller than the mesh size across most of the studied concentration range.

As an illustration, in Figure 10, we present the isotropic solution of rodlike DNA molecules (c = 0.3 mM) and their counterion atmospheres. At this concentration (0.3 mM), the mesh size should be 125 nm and DNA total persistence length 200 nm (due to very low salt conditions). Thus, on the level of the mesh cell DNA may be considered rodlike. The mesh size, probe length, and the thickness of the counterion atmosphere are shown to scale, illustrating that the occupied volume, even when enhanced by the atmosphere does not present a significant portion of the total available volume for diffusion of the probe DNA110*.

The occupied volume significantly influences the diffusion only for a tight mesh, where DNA110* probe is larger than the mesh size. There, however, the counterion concentration is high enough and the atmosphere thin enough that there is no distinction between systems in buffer or in very low salt. The distinction between the heterogeneous and homogeneous systems also disappears there as both systems are in the semidilute regime.

DNA Denaturation. The denaturation mechanism that affects probe DNA110* should also affect DNA146 and long DNA. For the homogeneous DNA110*/DNA146 system we identify denaturation of DNA110* from the increase in D_{110*}^{exp} below 0.02 mM. DNA146 solution may be taken as infinitely dilute below the concentration where the fits in Figure 7 merge—the occupied volume has no influence anymore. Thus, D_{110*}^{exp} reflects only DNA110* shape/conformation and indeed, ssDNA has a larger diffusion coefficient. Presumably, DNA146 denatures at similar concentrations as DNA110*, as the stability of DNA sequence is also related to its length.[54]

For the heterogeneous system DNA110*/long DNA and DNA110*/HA a pronounced D_{110*}^{exp} increase starts already below 0.2 mM (Figure 7, lower panel). As this increase is common for both heterogeneous systems, in principle it could only be due to a change in some common property. E.g., it could be a property of DNA110* present in both systems. However, we established just above that DNA110* denaturation only starts below 0.02 mM and may not be the origin of this increase. The only other common property of the two heterogeneous systems is the mesh size. Therefore, we argued that the said increase is due to opening of the mesh, Figure 9. Notwithstanding, we note that D_{110*}^{exp} increase for DNA110*/long DNA system starts only for 150 nm mesh size and for DNA110*/HA already for 100 nm mesh size. This slight difference may easily be within our experimental error, but the data points for long DNA do remain shifted, for a factor about 1.5, to higher mesh size values, throughout the increase range. This may be interpreted in the following manner. If long DNA denatures already in this region, it would present, for a given concentration n, a slightly tighter mesh than we calculated for the abscissa of Figure 9. That is, the number of chains and thus monomers doubles when strands break apart and monomer size b is also somewhat larger for single strands (0.43−0.5 nm instead of 0.34 nm[50]). Therefore, $(bn)_{\mathrm{dsDNA}}^{-1/2} \approx 1.7 \cdot (bn)_{\mathrm{ssDNA}}^{-1/2}$. This factor is very close to our estimate for the shift factor just above. While this analysis is speculative and the shift may well be due to an experimental error we also point to a feature in the dielectric spectroscopy data (see Supporting Information) that occurs in similar concentration range for the same long DNA samples (polydisperse salmon DNA). We take this as yet another indication of our long DNA samples denaturation below 0.2 mM. However, such a scenario where long DNA molecules would be less stable than short DNA fragments is in contradiction with studies showing that DNA will denature more easily if it is of shorter length.[54] Nevertheless, the issue of long DNA denaturation has no consequence on our argument that the pronounced D_{110*}^{exp} increase observed for heterogeneous systems is due to the mesh size becoming considerably larger (100−150 nm) than DNA110* fragment size (40 nm).

CONCLUSION

We remind the reader that the addition of salt suppresses the principal experimental feature of the semidilute polyelectrolytes, the SAXS correlation peak. This is due to the salt induced screening of the Coulomb interaction and the consequent suppression of the correlation hole around the chains. This change in solution structure (as if it *melts* away) occurs for rather high added salt levels of 0.1−1 M. Upon addition of salt, the density of chains does not change and the mesh size parameter itself should stay the same. It is only the correlation between the chains (the structure of the mesh) that goes away with the reduction in the counterion atmosphere extent due to added salt. The apparent difference in salt effect on structure and on the dynamics stems from the following: the counterion atmosphere contracts proportionally to κ^{-1} (defined by the added salt) while the OSF electrostatic contribution to the persistence length of chains goes away much sooner with κ^{-2}. So the mesh of rigid chains softens at 10 mM but the correlations among chains—the distinctive structure of the polyelectrolyte solution remain even above 0.1 M ionic strength.

In brief, in this work we probed the mesh formed by the semidilute solutions of semirigid polyelectrolytes. The basis for this study was to establish the equivalence between the correlation length obtained both from a structural method (SAXS) and a dynamics study (DS) and a simple geometrical parameter of the mesh size, across a broad concentration range. We established this both for DNA and HA, despite that HA lacks the characteristic polyelectrolyte peak in SAXS intensity curves. Having the size of the mesh measured, we probed the mesh by studying how the diffusion coefficient of a DNA fragment (of length comparable to the mesh size) deviates from its free diffusion value. It appeared that a mesh of similar properties is formed by a strong polyelectrolyte DNA and a weak polyelectrolyte HA in salt free solutions. In these salt free conditions electrostatic contribution to the persistence length is higher than the mesh size and HA and DNA polyions are rendered highly rigid. Thus, formed rigid mesh significantly impedes the diffusion of the probe fragment. Addition of salt *softens* the mesh, by reducing the persistence length below the mesh size and impedance to fragments diffusion is removed. We consider this effect (observed by studying the dynamics), to be complementary to the disappearance of the polyelectrolyte peak in SAXS intensity curves (a static, structural study) upon addition of salt.

dx.doi.org/10.1021/ma3021486 | Macromolecules 2013, 46, 1107−1118

APPENDIX A

We summarize some basic textbook concepts,[4,8] in order to provide a context for length-scale considerations presented in this work.

Screening Length. When we try to understand the distribution and thickness of the counterion atmosphere of a polyion, we use the concept of screening length(s) which depend on the ionic concentration and composition, e.g. Debye–Hückel screening length

$$\kappa^{-1} = \left(\frac{\varepsilon_0 \varepsilon_R k_B T}{2e^2}\right)^{1/2} I_s^{-1/2} \tag{11}$$

Here ε_0 is the permittivity of the vacuum, ε_R is the relative dielectric constant of the solvent, k_B is the Boltzmann constant, T is the temperature, e is the electron charge and I_s is the ionic strength of the solution. In order to estimate κ^{-1} for a polyelectrolyte without added salt, we take into account only the concentration of the counterions c_i and their valency z_i, so $I_s = c_i z_i^2$. Concentration of counterions stems from the monomer concentration, c of the polyelectrolyte, i.e., $c_i = cz_m/z_i$, where z_m is the number of charges a monomer carries (for double stranded DNA, $z_m = 2$, while for HA it is 1).

Bjerrum Length. The electrostatic interaction of two monovalent ions in a dielectric medium is comparable to k_BT at a distance $l_B = (e^2/(4\pi\varepsilon_0\varepsilon_R k_B T))$. In water, the Bjerrum length is $l_B = 0.72$ nm. In other words, in water two monovalent ions effectively cease to interact beyond this distance.

Chain Size. A polyion of a polymerization degree N, with monomer size b, has a contour length $L_c = Nb$. Chain size R is the measure of the maximum spatial extent of the polyion chain. It is smaller than the contour length if the polyion is coiled. The minimum extent occurs if the polyion is so flexible that each of its monomers may be regarded as a step in a random walk, then $R = bN^{1/2}$.

Persistence Length. L_p is a measure of the stiffness of the polymer chain. In a polyelectrolyte, the total persistence length $L_p = L_0 + L_e$ is a combination of the structural L_0 and the electrostatic contribution L_e. The latter is due to the Coulombic repulsion of the charged groups found along the chain, which renders the chain more rigid and tends to extend it. As this interaction is screened by the added salt the models for L_e must include the added salt concentration, usually via κ^{-1}.[52] A frequently used model to calculate L_e is Odijk-Skolnick-Fixman model:[55,56] $L_e = (1/(4\kappa^2 l_B))$. The electrostatic contribution may easily surpass the structural one in very low salt conditions. A polyion will behave as a rod if the persistence length is comparable to the contour length, $L_p \approx L_c$.

Dilute Solution, Polyelectrolyte concentration is so low that the polyions are set apart, i.e. their average distance d is larger than the chain size or the contour length, L_c of a polyion. An average volume taken by a polyion scales inversely with polyion concentration $d^3 \propto 1/c_p$. The latter is related to c, the monomer concentration – $c_p = c/N$ and thus $d = (c/N)^{-1/3}$.[14,17,25]

Dilute–Semidilute Crossover Concentration. As the polyelectrolyte concentration is raised, the average distance gets reduced and eventually becomes comparable to the chain size or the contour length of the polyion, $d \approx L_c$. This occurs at a crossover concentration $c^* = N/L_c^3$.

Semidilute Solution. Polyions start to overlap. The principal characteristic of a semidilute solution is that there is no way to distinguish whether two neigboring polyion segments, belong to the same chain or different ones—in other words, the chains lose identity. Correspondingly, average distance between the chains or chain size, as well as the contour length are not relevant length scales to describe a semidilute solution.

de Gennes Correlation Length. For a semidilute solution, any relevant length scale ξ should scale in some manner with polyelectrolyte (monomer) concentration, $\xi \propto c^m$, and not with the chain size R or polymerization degree N. Such a length scale should also become, at the crossover concentration c^*, comparable to chain size R, where the latter is comparable to the distance between the chains d. Therefore, we should have $\xi \propto R(c/c^*)^m$. Since $R \approx d \approx L_c = Nb$ and $c^* = N/L_c^3$, we need to set the exponent $m = -1/2$ to avoid dependence of ξ on N. Thus, we get a length scale relevant for describing a semidilute solution which scales with the square root of the monomer concentration, $\xi \propto c^{-1/2}$. This scaling approach was introduced by de Gennes et al.[20] in association with the isotropic phase model.

APPENDIX B

Experimental details of dielectric spectroscopy (DS) technique applied to long DNA or HA samples are described in more detail elsewhere.[18,33] As DS results are an important reference here we describe the technique in the following. In brief, a sample solution droplet of 100 μL is applied between platinum electrodes of a homemade capacitive chamber. The chamber is closed and connected to the temperature control unit and the Agilent 4294A precision impedance analyzer which operates in the frequency range 100 Hz-100 MHz. The complex conductivity spectrum of the sample is subtracted for the spectrum of NaCl solution with a similar free ionic conductivity. The resulting spectrum is converted into the complex dielectric function and fitted in a complex plane. The principal fit parameter of interest here is the mean relaxation time τ_0.

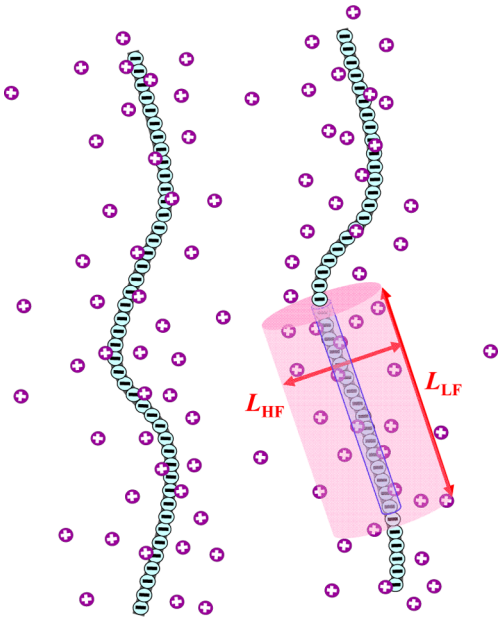

Figure 11. External electric field induces a dipole formed by the polyion and the counterion atmosphere. Dipoles induced perpendicular or along the polyion chain would have different relaxation times, due to different length scales involved.

dx.doi.org/10.1021/ma3021486 | *Macromolecules* 2013, 46, 1107–1118

That is, the applied small ac electric field induces a dipole formed by counterion atmosphere oscillating in relation to the polyion, Figure 11. The relaxation time τ_0 of the induced dipole necessarily corresponds to their size., i.e. to the associated length scale L *via* Einstein−Smoluchowski diffusion equation $L^2 \propto \tau_0 D_{in}$, where D_{in} is the diffusion constant of counterions.[57] The equation is applied since the counterion displacements take place by diffusive motion.

■ ASSOCIATED CONTENT

Supporting Information

More detailed discussion of the features of the scattering intensity curves for HA, further arguments for the length scale obtained by dielectric spectroscopy to be the correlation length, as well as the fact that it attains realistic values when rescaled by 2π. This material is available free of charge via the Internet at http://pubs.acs.org/.

■ AUTHOR INFORMATION

Corresponding Author

*E-mail: tvuletic@ifs.hr.

Notes

The authors declare no competing financial interest.

■ ACKNOWLEDGMENTS

We gratefully acknowledge F. Livolant for a generous supply of mononucleosomal DNA146 samples and J. Rädler for providing access to his FCS instrument. This work is primarily based on the support from the Unity through Knowledge Fund, Croatia, under Grant 22/08. We were also supported by S. Tomić both through fruitful discussions and with material help within her Project No. 035-0000000-2836 by the Croatian Ministry of Science, Education, and Sports.

■ REFERENCES

(1) Oosawa, F. *Polyelectrolytes*; Marcel Dekker; New York, 1971, Chapter 5.
(2) Hara, M., Ed. *Polyelectrolytes*; Dekker; New York, 1993.
(3) Rubinstein, M., Colby, R. H. *Polymer Physics*; Oxford University Press: Oxford, U.K., 2003.
(4) van der Maarel, J. R. C. *Introduction to Biopolymer Physics*; World Scientific; Singapore, 2007.
(5) Holm, C., Kekicheff, P., Podgornik, R., Eds. *Electrostatic Effects in Soft Matter and Biophysics*; Vol. *46* of NATO Science Series II: Mathematics, Physics and Chemistry; Kluwer Academic Press; Dordrecht, The Netherlands, 2001.
(6) Manning, G. S. *Q. Rev. Biophys.* **1978**, *11*, 179.
(7) Manning, G. S. *J. Chem. Phys.* **1969**, *51*, 924.
(8) Dobrynin, A. V.; Rubinstein, M. *Prog. Polym. Sci.* **2005**, *30*, 1049.
(9) Rubinstein, M.; Colby, R. H.; Dobrynin, A. V. *Phys. Rev. Lett.* **1994**, *73*, 2776.
(10) Deserno, M. *Eur. Phys. J. E* **2001**, *6*, 163.
(11) Deshkovski, A.; Obukhov, S.; Rubinstein, M. *Phys. Rev. Lett.* **2001**, *86*, 2341.
(12) Kanduč, M.; Naji, A.; Podgornik, R. *J. Chem. Phys.* **2010**, *132*, 224703.
(13) Schmidt, C. F.; Bäermann, M.; Isenberg, G.; Sackmann, E. *Macromolecules* **1989**, *22*, 3638.
(14) Kaji, K.; Urakawa, H.; Kanaya, T.; Kitamaru, R. *J. Phys. (Fr.)* **1988**, *49*, 993.
(15) Koch, M. H. J.; Sayers, Z.; Sicre, P.; Svergun, D. *Macromolecules* **1995**, *28*, 4904.
(16) Keyser, U. F.; Koeleman, B. N.; van Dorp, S.; Krapf, D.; Smeets, R. M. M.; Lemay, S. G.; Dekker, N. H.; Dekker, C. *Nature Phys.* **2006**, *2*, 473.
(17) Ito, K.; Yagi, A.; Ookubo, N.; Hayakawa, R. *Macromolecules* **1990**, *23*, 857.
(18) Tomić, S.; Dolanski Babić, S.; Vuletić, T.; Krča, S.; Ivanković, D.; Griparić, L.; Podgornik, R. *Phys. Rev. E* **2007**, *75*, 021905.
(19) Vuletić, T.; Dolanski Babić, S.; Grgičin, D.; Aumiler, D.; Rädler, J.; Livolant, F.; Tomić, S. *Phys. Rev. E* **2011**, *83*, 041803.
(20) de Gennes, P.-G.; Pincus, P.; Velasco, R. M.; Brochard, F. *J. Phys. (Paris)* **1976**, *37*, 1461.
(21) Odijk, T. *Macromolecules* **1979**, *12*, 688.
(22) Nierlich, M.; Williams, C. E.; Boue, F.; Cotton, J. P.; Daoud, M.; Farnoux, B.; Jannink, G.; Picot, C.; Moan, M.; Wol, C.; Rinaudo, M.; de Gennes, P.-G. *J. Phys. (Fr.)* **1979**, *40*, 701.
(23) Koyama, R. *Macromolecules* **1984**, *17*, 1594.
(24) Koyama, R. *Physica B* **1983**, *120*, 418.
(25) Wang, L.; Bloomfield, V. A. *Macromolecules* **1991**, *24*, 5791.
(26) Strzelecka, T. E.; Rill, R. L. *Macromolecules* **1991**, *24*, 5124.
(27) Buhler, E.; Boue, F. *Macromolecules* **2004**, *37*, 1600.
(28) Combet, J.; Isel, F.; Raviso, M.; Boue, F. *Macromolecules* **2005**, *38*, 7456.
(29) Zustiak, S. P.; Nossal, R.; Sackett, D. L. *Biophys. J.* **2011**, *101*, 255.
(30) Jena, S. S.; Bloomfield, V. A. *Macromolecules* **2005**, *38*, 10551. Busch, N. A.; Kim, T.; Bloomfield, V. A. *Macromolecules* **2000**, *33*, 5932.
(31) Baumann, C. G.; Smith, S. B.; Bloomfield, V. A.; Bustamante, C. *Proc. Natl. Acad. Sci. U.S.A.* **1997**, *94*, 6185.
(32) Buhler, E.; Boue, F. *Eur. Phys. J. E* **2003**, *10*, 89.
(33) Vuletić, T.; Dolanski Babić, S.; Ivek, T.; Grgičin, D.; Tomić, S.; Podgornik, R. *Phys. Rev. E* **2010**, *82*, 011922.
(34) Tomić, S.; Dolanski Babić, S.; Ivek, T.; Vuletić, T.; Krča, S.; Livolant, F.; Podgornik, R. *Europhys. Lett.* **2008**, *81*, 68003.
(35) Cowman, M. K.; Matsuoka, S. *Carbohydr. Res.* **2005**, *340*, 791.
(36) Tomić, S.; Grgičin, D.; Ivek, T.; Vuletić, T.; Dolanski Babić, S.; Podgornik, R. *Physica B* **2012**, *407*, 1958.
(37) Villetti, M.; Borsali, R.; Diat, O.; Soldi, V.; Fukada, K. *Macromolecules* **2000**, *33*, 9418.
(38) Sikorav, J.-L.; Pelta, J.; Livolant, F. *Biophys. J.* **1994**, *67*, 1387.
(39) Strzelecka, T. E.; Rill, R. L. *J. Am. Chem. Soc.* **1987**, *109*, 4513.
(40) Carl Zeiss: Applications Manual LSM 510 - ConfoCor 2 Application Handbook
(41) Tirado, M. M.; Martinez, C. L.; de la Torre, J. G. *J. Chem. Phys.* **1984**, *81*, 2047.
(42) Stellwagen, E.; Stellwagen, N. C. *Biophys. J.* **2003**, *84*, 1855.
(43) Borsali, R.; Nguyen, H.; Pecora, R. *Macromolecules* **1998**, *31*, 1548.
(44) Hayter, J.; Janninck, G.; Brochard-Wyart, F.; de Gennes, P.-G. *J. Phys., Lett.* **1980**, *41*, 451.
(45) Castelletto, V.; Itri, R.; Amaral, L. Q.; Spada, G. P. *Macromolecules* **1995**, *28*, 8395.
(46) Nishida, K.; Kaji, K.; Kanaya, T. *J. Chem. Phys.* **2001**, *114*, 8671.
(47) Dhont, J. K. G.; Van Bruggen, M. P. B.; Briels, W. J. *Macromolecules* **1999**, *32*, 3809.
(48) Wilk, A.; Gapinski, J.; Patkowski, A.; Pecora, R. *J. Chem. Phys.* **2004**, *121*, 10794.
(49) Record, M. T., Jr. *Biopolymers* **1975**, *14*, 2137.
(50) Tinland, B.; Pluen, A.; Sturm, J.; Weill, G. *Macromolecules* **1997**, *30*, 5763.
(51) Sorci, G. A.; Reed, W. F. *Macromolecules* **2002**, *35*, 5218.
(52) Ullner, M. *J. Chem. Phys.* **2003**, *107*, 8097.
(53) Maret, G.; Weill, G. *Biopolymers* **1983**, *22*, 2727.
(54) Buyukdagli, S.; Joyeux, M. *Phys. Rev. E* **2007**, *78*, 021917.
(55) Odijk, T. *J. Polym. Sci., Polym. Phys. Ed.* **1977**, *15*, 477.
(56) Skolnick, J.; Fixman, M. *Macromolecules* **1977**, *10*, 944.
(57) Bordi, F.; Cametti, C.; Colby, R. H. *J. Phys.: Condens. Matter* **2004**, *16*, R1423.